ACCOUNTS
of chemical research

Zeolite Membranes: Microstructure Characterization and Permeation Mechanisms

MIAO YU,* RICHARD D. NOBLE,* AND JOHN L. FALCONER

Department of Chemical and Biological Engineering, University of Colorado, Boulder, Colorado 80309-0424, United States

RECEIVED ON MARCH 14, 2011

CONSPECTUS

Since their first synthesis in the 1940s, zeolites have found wide applications in catalysis, ion-exchange, and adsorption. Although the uniform, molecular-size pores of zeolites and their excellent thermal and chemical stability suggest that zeolites could be an ideal membrane material, continuous polycrystalline zeolite layers for separations were first prepared in the 1990s. Initial attempts to grow continuous zeolite layers on porous supports by in situ hydrothermal synthesis have resulted in membranes with the potential to separate molecules based on differences in molecular size and adsorption strength. Since then, further synthesis efforts have led to the preparation of many types of zeolite membranes and better quality membranes. However, the microstructure features of these membranes, such as defect size, number, and distribution as well as structure flexibility were poorly understood, and the fundamental mechanisms of permeation (adsorption and diffusion), especially for mixtures, were not clear. These gaps in understanding have hindered the design and control of separation processes using zeolite membranes.

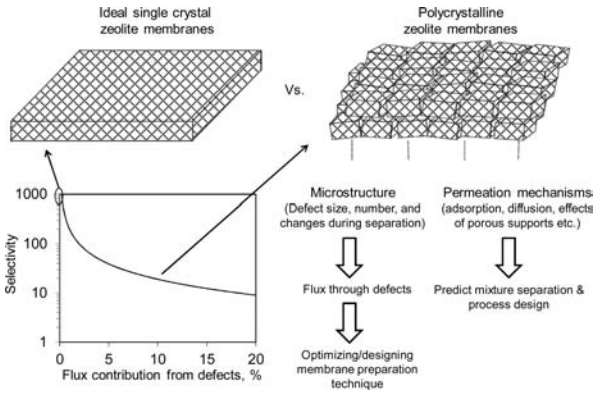

In this Account, we describe our efforts to characterize microstructures of zeolite membranes and to understand the fundamental adsorption and diffusion behavior of permeating solutes. This Account will focus on the MFI membranes which have been the most widely used but will also present results on other types of zeolite membranes.

Using permeation, x-ray diffraction, and optical measurements, we found that the zeolite membrane structures are flexible. The size of defects changed due to adsorption and with variations in temperature. These changes in defect sizes can significantly affect the permeation properties of the membranes. We designed methods to measure mixture adsorption in zeolite crystals from the liquid phase, pure component adsorption in zeolite membranes, and diffusion through zeolite membranes. We hope that better understanding can lead to improved zeolite membranes and eventually facilitate the large-scale application of zeolite membranes to industrial separations.

1. Introduction

Zeolites are an ideal membrane material because they have uniform, molecular-size pores (usually 0.3−1.3 nm) and excellent thermal, mechanical, and chemical stability. Some zeolites have been synthesized into thin, polycrystalline membranes. Figure 1 shows scanning electron microcsopy (SEM) images of the top and cross section of a typical MFI zeolite membrane composed of intergrown crystals. Since zeolite pores are usually of molecular size, a space between crystals that is only 2 or 3 nm is sufficient to dramatically degrade membrane separation properties because molecular diffusivities decrease exponentially as their sizes approach the pore size. Thus, preparing high quality zeolite membranes is challenging. Excellent separation performance was demonstrated for various mixtures, including those difficult to separate by other methods, such as organic isomers[1−5] and close-boiling point mixtures.[6] Separations under high temperature and pressure conditions[7,8] and chemically challenging conditions[9] demonstrated the potential and versatility of zeolite membranes.

Although more than 190 distinct framework zeolite structures are known, less than 20 have been prepared as

Published on the Web 08/02/2011 www.pubs.acs.org/accounts
10.1021/ar200083e

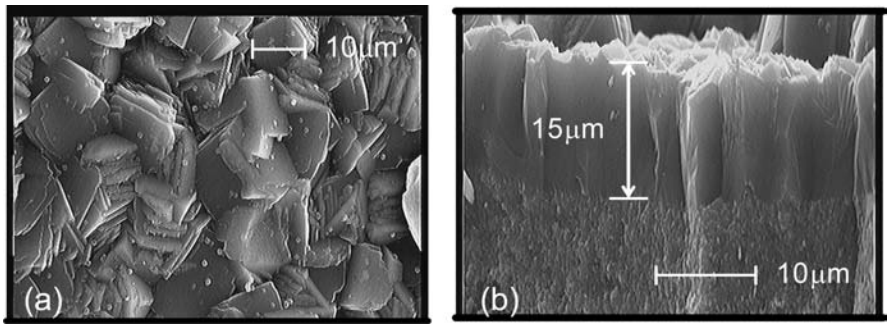

FIGURE 1. SEM images of MFI zeolite membrane grown on porous alumina support: (a) top view and (b) side view. Reproduced with permission from ref 69. Copyright 2007 John Wiley and Sons.

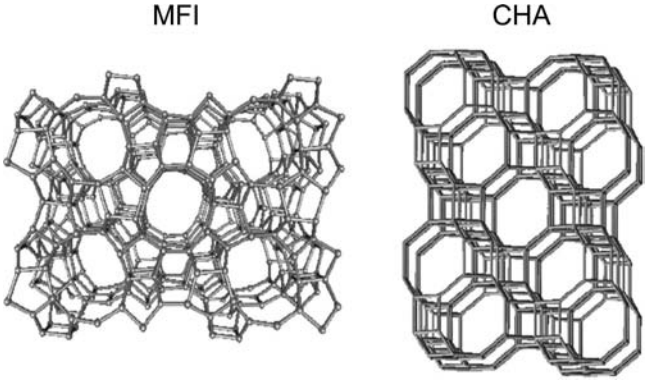

FIGURE 2. Atomic stick representations of MFI (silicalite-1, ZSM-5) and CHA (SAPO-34) zeolite structure frameworks. Nodes represent tetrahedral framework atoms and sticks represent oxygen bridges.[102]

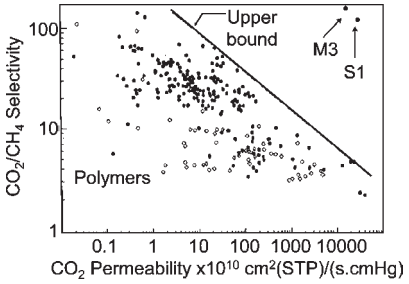

FIGURE 3. Comparison of CO_2/CH_4 separation selectivity versus CO_2 permeability for polymeric and SAPO-34 membranes M3 and S1 at 295 K and feed and permeate pressures of 222 and 84 kPa, respectively. Thicknesses of membranes M3 and S1 were 5 and 2.5 μm, respectively (estimated from SEM images of the cross section of broken membranes). Reproduced with permission from 8. Copyright 2006 John Wiley and Sons.

membranes that demonstrate significant separation selectivity, and large variations in separation performance were reported. Difficulty of preparing zeolite membranes with high selectivities is mainly attributed to the existence of defects and lack of controllable methods to minimize them. Defects are intercrystalline spaces (sometimes called nonzeolitic pores) that are larger than zeolite pores. To take advantage of molecular-sieving and preferential adsorption properties of zeolite pores, both defect number and size must be minimized to reduce flux through defects. We conducted extensive studies on zeolite membrane synthesis and mixture separations.[1−6,9−56] We prepared more than 10 types of zeolite membranes, with the main emphasis on membranes with MFI and CHA structures (Figure 2). SAPO-34 membranes (aluminum and phosphate-substituted CHA) efficiently remove CO_2 from CH_4 under high pressure (~7 MPa) and show significantly better CO_2 separation performance than polymeric membranes,[8] shown in Figure 3. SAPO-34 membranes have great potential for large-scale application in natural gas purification.

Some excellent reviews were published on different aspects of zeolite membranes.[57−64] Here, we review our zeolite membrane research and provide insights on microstructure (defect size and number and how they change under permeation conditions) and how it affects permeation/separation and separation mechanisms.

2. Microstructure/Defects Characterization

Defects are defined as intercrystalline spaces that are larger than zeolite pores. Defects, which are inevitable in polycrystalline zeolite membranes, usually have lower selectivities and should be minimized by optimizing membrane preparation and/or by selectively blocking them. Characterizing microstructure (defect size, number/concentration, and changes under various conditions) and evaluating their contribution to the total flux are important for evaluating membrane preparation methods and materials that selectively block defects. Our research on defect characterization has mainly focused on MFI zeolite membranes, and we used various permeation measurements initially to attempt to determine the defect contribution to zeolite membrane transport. These include

(i) measuring the ratio of single-gas permeances, such as N_2/SF_6,[13−15,65,3,17,4,18,5,20,21] *n*-butane/*i*-butane,[10,16,18,21−23,9,24,26−31,7,66,67] and H_2/i-butane;[11,16,17,21,22,26,28,30]

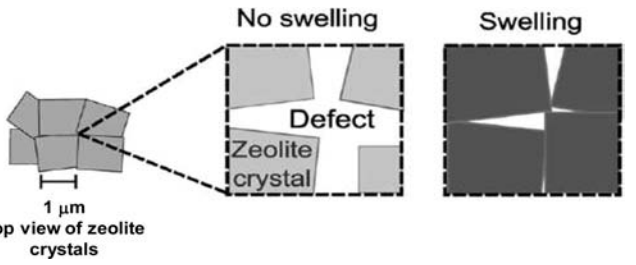

FIGURE 4. Schematic diagram showing zeolite crystal expansion upon adsorption and corresponding shrinkage of a nanometer-sized defect. Reproduced with permission from ref 78. Copyright 2010 Elsevier.

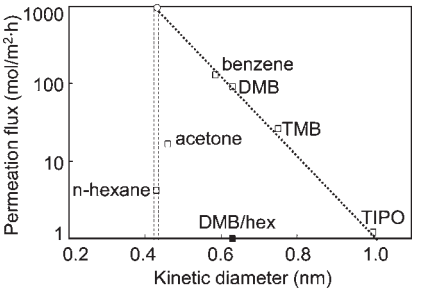

FIGURE 5. Pervaporation flux through a MFI membrane (B-ZSM-5) (300 K) versus kinetic diameter of the permeating molecule as pure components (open squares), DMB flux in mixture with 4% *n*-hexane (solid square). Reproduced with permission from ref 69. Copyright 2007 John Wiley and Sons.

(ii) measuring the flux of molecules that are significantly larger than MFI pores, such as 1,3,5-triisopropylbenzene (TIPB),[25,27,31] isooctane,[6,2] 2,2-dimethylbutane (DMB),[31,68,69] and 1,3,5-trimethylbenzene (TMB);[68,69]

(iii) mixture separations, such as organic isomers (*n*-butane/*i*-butane[3,9,16,18,20,21,28,30,67] and *n*-hexane/DMB[3−5,7,28,70,71]), where larger isomers effectively cannot fit into or have difficulty entering zeolite pores;

(iv) permporosimetry,[72−79] where the flux of a non-adsorbing gas is measured as the activity of an adsorbing molecule in the feed increases.

Many of these methods did not account for the flexible nature of the zeolite structure, so they may not yield accurate characterizations of defect properties or membrane quality.

2.1. Zeolite Membranes Are Flexible. The characterization methods described in the previous section were used to determine the defects contribution to membrane transport. They implicitly assume that zeolite membrane structures are rigid. Our recent studies clearly demonstrated, however, that MFI and A structures are sufficiently flexible that defect sizes can decrease or increase when certain molecules adsorb in the zeolite pores,[68,69,72−81] shown schematically in Figure 4 for crystal expansion.[78] For example, defect sizes in MFI membranes were initially concluded to decrease upon *n*-hexane adsorption in MFI pores because of the following experimental measurements:

(1) Fluxes of molecules too large to adsorb in MFI pores, such as DMB and isooctane, were more than 2 orders of magnitude larger than the *n*-hexane flux during single-component pervaporation (Figure 5), although *n*-hexane is significantly smaller than these molecules and it absorbs in MFI pores.[68,69]

(2) Permporosimetry using *n*-hexane and benzene as condensable hydrocarbons gave dramatically different results. Both molecules can block helium permeation through MFI pores when their loadings are high, but helium fluxes can differ by more than 3 orders of magnitude for the membrane with small defects (membrane 2 in Figure 6a). For a MFI membrane with larger defects, *n*-hexane had a smaller effect, but the helium flux when *n*-hexane adsorbed was 2/3 of the helium flux when benzene adsorbed (membrane 1 in Figure 6a).[72] Helium flux is lower for membrane 2 when *n*-hexane adsorbs because it expands the MFI crystals and shrinks defect sizes. Permporosimetry measurements suggest that other molecules (SF_6, propane, *n*-butane, *n*-pentane) also expand MFI crystals and shrink defect sizes (Figure 6b).

(3) Defect volume, indicated by the amount of adsorbed DMB (a molecule that adsorbs in defects but is too large to adsorb in the MFI pores) decreased by 50% when 0.7% *n*-hexane was added to DMB.[80]

(4) DMB or 1,3,5-trimethylbutane (TMB) flux (molecules larger than MFI pores) decreased an order of magnitude or more when low concentrations (less than 1%) of *n*-hexane were added to the feed (Figure 7).[68]

Further studies showed that adsorption of many molecules in MFI pores also expanded zeolite crystals and reduced defects size in MFI membranes.[68,69,73,74] Lee et al.[73] observed this behavior for SF_6 and *n*-C_3−*n*-C_6; SF_6-induced expansion stopped 99% of the flux through defects of a B-ZSM-5 (boron-substituted MFI) membrane with a large number of small defects, whereas for a silicalite-1 (all-silica MFI) membrane with larger defects SF_6 only decreased the flux through defects by 30%. Sorenson and co-workers[74,76,79,81] studied zeolite crystal expansion by optical microscopy for large silicalite-1 crystals and powder X-ray diffraction (XRD) for small crystals and reported that crystal expansion changed permeation and separation properties of zeolite membranes. Silicalite-1 crystals expanded upon adsorption of C_4−C_8 alkanes and *i*-butane at room temperature, and

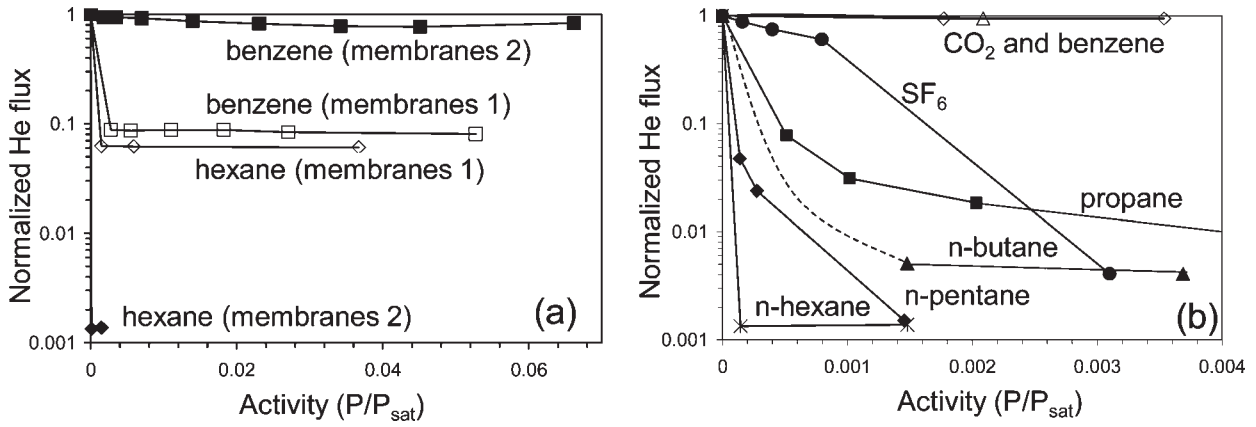

FIGURE 6. Normalized helium flux (room temperature) as function of hydrocarbon activity for MFI membranes 1 (silicalite-1) and 2 (B-ZSM-5) for benzene and hexane (a) and for membrane 2 for CO_2, benzene, SF_6, propane, n-butane, n-pentane and *n*-hexane at very low activity (b) added to the feed during permporosimetry. Reproduced with permission from ref 72. Copyright 2008 American Chemical Society.

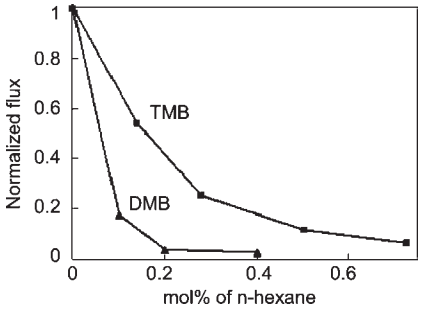

FIGURE 7. Normalized 2,2-dimethylbutane (DMB) and 1,3,5-trimethylbutane (TMB) pervaporation fluxes through a MFI membrane (300 K) as a function of the *n*-hexane feed concentration. Pure DMB flux was 91.3 mol/(m^2·h) and pure TMB flux was 26.3 mol/(m^2·h). Reproduced with permission from ref 68. Copyright 2007 Elsevier.

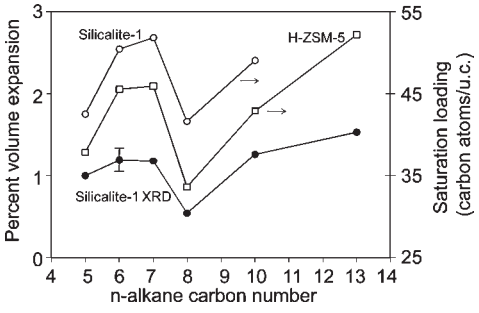

FIGURE 8. Percent volume expansion of silicalite-1 unit cell (298 K) due to *n*-alkane adsorption, measured by XRD, and saturation loading of *n*-alkanes (carbon atoms/uc) versus *n*-alkane carbon number. Reproduced with permission from ref 74. Copyright 2008 American Chemical Society.

expansion was nonisotropic. Powder XRD showed that silicalite-1 crystals expanded 0.2−0.45% in the *c*-direction, and the same expansion was also observed by optical microscopy of 200 μm crystals. Powder XRD showed that crystals expanded ~0.5% in the *b*-direction and 0.2- 0.45% in the *a*-direction.[74]

Transient permeation measurements showed that crystal expansion by *n*-C_6 and *n*-C_8 adsorption decreased defect pore sizes in MFI membranes, even at loadings lower than 10% of saturation.[74] XRD studies determined that alcohols and *n*-alkanes (C_5−C_{13}) expanded silicalite-1; percent volume expansion at saturation loadings of *n*-alkanes correlated linearly with the number of carbon atoms per unit cell, and tridecane expanded silicalite-1 the most (1.53 vol %) (Figure 8). Pervaporation isooctane flux, which is larger than silicalite-1 pores and only permeates through defects, decreased about 2 orders of magnitude upon addition of *n*-alkanes, with the larger decreases for molecules that expanded the crystals more (Table 1).[76] Since many of the larger molecules used for characterizing MFI membranes (e.g., SF_6, *n*-hexane) in the literature expand MFI crystals, whereas the smaller molecules (H_2, He, N_2) do not, single gas permeance ratios, mixture separation selectivities, and permporosimetry results using *n*-hexane may not reflect MFI membrane quality. Defect sizes changed during these measurements, and estimated membrane quality depended on which molecules were used for characterization. Powder XRD measurements also showed unit cell changes of B-ZSM-5 and SAPO-34 crystals upon adsorption of different molecules and at different loadings,[79] and permeation measurements showed consistent results between changes in the zeolite unit cell volumes of B-ZSM-5 and permeation fluxes through zeolite membrane defects (Figure 9).

Although most adsorbates investigated expanded zeolite crystals and expansion increased monotonically with loading, some molecules contracted crystals at low loading and expanded them at higher loadings. For example, *i*-butane caused this behavior for B-ZSM-5 crystals[79] (Figure 9b) and

TABLE 1. Isooctane/*n*-Alkane Mixture Pervaporation through Two MFI Zeolite Membranes (B-ZSM-5) (313 K)[76]

membrane			n-C_6	n-C_7	n-C_8	n-C_{10}	n-C_{13}
A	feed wt % isooctane	100	98.6	98.7	94.0	98.4	99.4
	isooctane flux (mol/m^2·h)	17.9	0.29	0.25	0.88	0.3	0.13
B	feed wt % isooctane	100	99.4	97.9	99.2	98.0	99.5
	isooctane flux (mol/m^2·h)	14.0	0.59	0.7	1.18	0.48	0.19

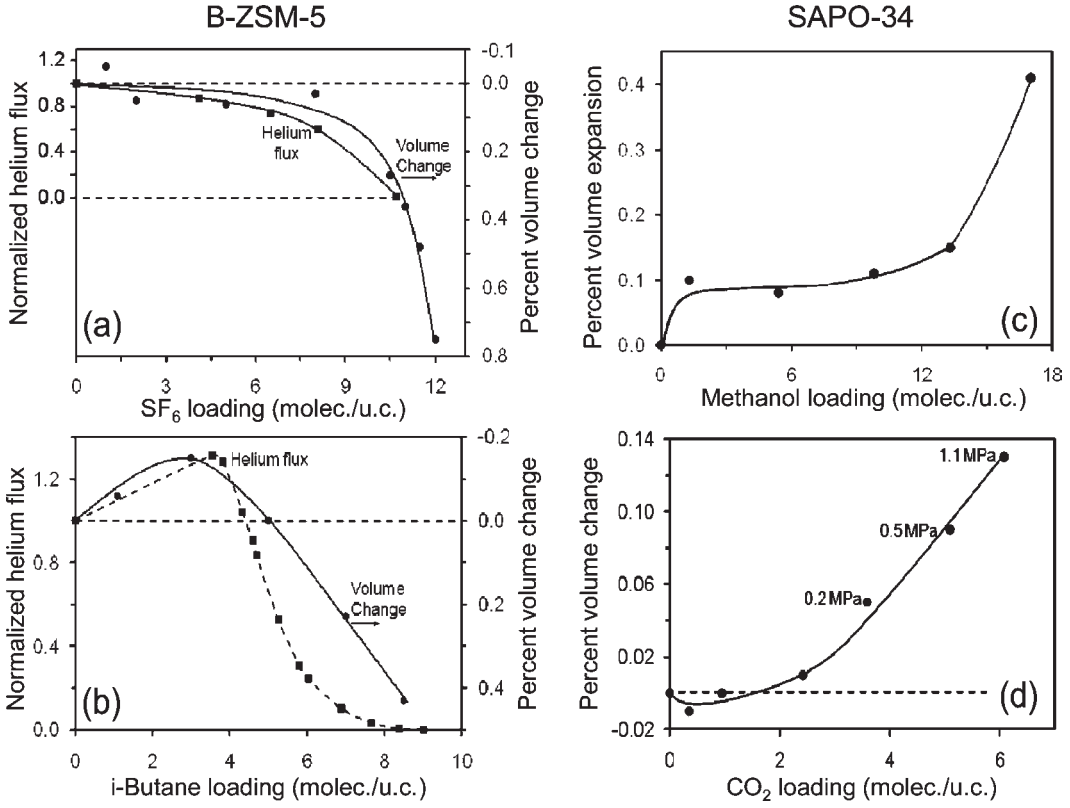

FIGURE 9. Normalized helium flux during permporosimetry for B-ZSM-5 membrane (room temperature) and percent volume change of B-ZSM-5 crystals (300 K), measured by XRD, as a function of SF_6 (a) and *i*-butane (b) loading, and percent volume expansion of SAPO-34 crystals (300 K), measured by XRD, as function of methanol (c) and CO_2 (d) loading. Reproduced with permission from ref 79. Copyright 2010 Elsevier.

water caused this behavior for zeolite A crystals[81] (Figure 10). Sorenson et al.[81] found using powder XRD that, at thermodynamic activity of 0.03, water contracted NaA zeolite by 0.22 vol % and increased helium flux through a NaA membrane by about 80% (Figure 10); it also increased the *i*-butane vapor flux by 14% and *i*-propanol (IPA) pervaporation flux by 25%. At activities above 0.07, water expanded NaA crystals and correspondingly decreased the fluxes of helium, *i*-butane, and IPA through the NaA membrane. They concluded that the observed high pervaporation selectivities for water/alcohol separations in zeolite A membranes were due, at least partially, to water-induced expansion of NaA crystals.

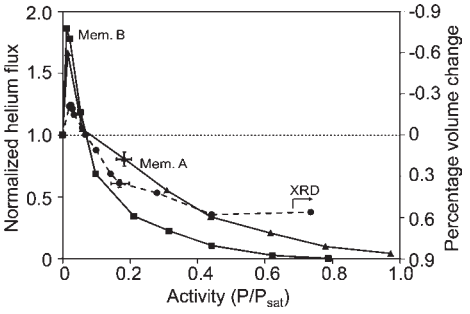

FIGURE 10. Normalized helium flux for two NaA zeolite membranes and NaA unit cell percent volume change (300 K) (XRD measurements; dashed line), plotted with its axis inverted, as a function of water activity. Reproduced with permission from ref 79. Copyright 2010 Elsevier.

Observed permeation results were not due to capillary condensation, which could not occur at low activities where crystal expansion and contraction were observed. Another explanation that might be proposed for the above results

instead of crystal expansion is preferential adsorption (e.g., of *n*-hexane) but this does not explain many of the results. For example, it cannot explain why the DMB flux was 2 orders of magnitude higher than *n*-hexane,[68,69] nor can it explain how *i*-butane adsorption increased the helium flux through a membrane. However, crystal contraction can explain this;[79] It also cannot explain why adsorbing a large molecule in the defects increased the SF_6 flux (as much as a factor of 6) but decreased H_2 flux.[78] These studies clearly showed that polycrystalline zeolite membranes are flexible and their defect sizes change due to the adsorbate-induced crystal expansion and contraction.

2.2. Defect Sizes and Volume Fraction. Capillary condensation during permeation measurements, combined with appropriate physical models (Kelvin and Horvath−Kawazoe (H−K) equations), were used to estimate defect sizes. Two methods, vapor permeation and permporosimetry, were used to determine defect sizes in MFI zeolite membranes. Vapor permeation was used to estimate defect sizes in MFI zeolite membranes.[68,69,72] Molecules were used that were too large to adsorb in MFI pores at a measurable rate and were assumed to only permeate through defects. Total pressure drop across the membrane was zero during vapor permeation measurements because a pressure drop inhibited vapor condensation in defects and thus overestimated defect sizes.[77] Isooctane and DMB were used because they have reasonable vapor pressures, but have kinetic diameters of 0.70 and 0.63 nm and thus do not readily adsorb in the 0.6-nm MFI pores, particularly at room temperature.[82] The activity (or partial pressure) where capillary condensation took place was identified by a sharp flux increase and used to estimate the defect size distribution. Although absolute defect sizes are only estimates, they provide a good measure of relative sizes for different membranes. DMB vapor permeation estimated the pores to be in the 2.5−4 nm range for MFI membranes used.[68,69] Isooctane vapor permeation indicated that average defect size decreased from approximately 3.0 to 1.5 nm as temperature increased from 300 to 348 K, apparently due to thermal expansion of MFI crystals.[72] The H−K model was used to estimate defect size, since this model was developed for slit type pores and boundaries between MFI single crystals were assumed to be slits. This measurement, however, does not rule out smaller pores, in which capillary condensation does not occur because their sizes are less than several molecular diameters.

Permporosimetry, using *n*-hexane with a pressure drop across the membrane, has been used to estimate defect sizes, utilizing capillary condensation in defects to block He or N_2 permeation.[72−79] However, these defect size distributions should be re-evaluated because (1) defect sizes shrink when *n*-hexane adsorbs in MFI pores;[68,69,72,76] (2) a pressure drop across the membrane significantly inhibits condensation in defects (Figure 11).[77] Tokay et al.[77] used water, benzene, and DMB as condensing molecules and conducted permeation measurements under low or zero pressure drop to avoid these two issues. Benzene and water have negligible effects on the MFI crystal size and DMB cannot enter MFI pores. Condensed liquids are more stable in defects at low pressure drop. They estimated average defect size to be about 2 nm for a MFI membrane.

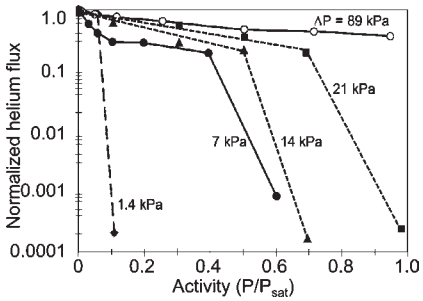

FIGURE 11. Normalized helium flux as function of water thermodynamic activity at different pressure drops during permporosimetry for a MFI membrane (B-ZSM-5) (room temperature). Reproduced with permission from ref 79. Copyright 2010 Elsevier.

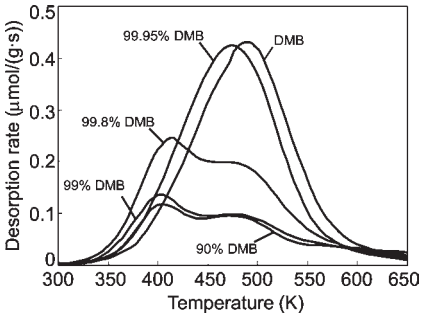

FIGURE 12. TPD profiles of DMB from MFI membrane after adsorption of DMB and *n*-C_6/DMB liquid mixtures. Reproduced with permission from ref 80. Copyright 2008 Elsevier.

Temperature-programmed desorption (TPD) was used to characterize the defect volume directly in MFI membranes by measuring the adsorbed DMB amount at room temperature.[80] As the *n*-hexane amount in the liquid increased, the DMB amount desorbing decreased significantly, even for 0.2% *n*-hexane (Figure 12). Dimethylbutane was used because it is only slightly larger than MFI pores and thus can probe defects that decrease selectivity in MFI membranes; it can adsorb in MFI pores, but adsorption is so slow

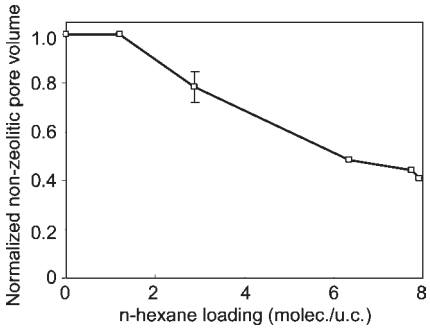

FIGURE 13. Nonzeolitic pore volume in an MFI membrane, normalized by nonzeolitic pore volume when no *n*-hexane was adsorbed, versus the *n*-hexane loading in the MFI crystals. Reproduced with permission from ref 80. Copyright 2008 Elsevier.

at room temperature that essentially none adsorbs on the measurement time scale.[83,82] Thus, any DMB adsorbed at room temperature in a MFI membrane is adsorbed in the defects, and the amount adsorbed was assumed to be a good measure of defect volume. Defect volume percentage of a MFI membrane that had 26% of its helium flux through defects was estimated to be 2.8%, from the DMB amount that desorbed and from the *n*-hexane amount that desorbed (for total zeolite crystal volume). Change in the DMB amount adsorbed was used to determine the change in defect volume caused by crystal expansion when *n*-hexane/DMB mixtures were used. Figure 13 shows the normalized defect volume change as *n*-hexane loading in the MFI pores increased. At saturation loading of *n*-hexane, defect volume decreased to about 40% of that without *n*-hexane in zeolite pores, directly showing adsorbate-induced crystal expansion decreased defect sizes.

3. Adsorption and Diffusion in Zeolite Crystals and Membranes

Zeolite membranes separate mixtures by differences in adsorption and diffusion rates and, in some cases, by molecular sieving. Transport through zeolite membrane pores occurs by an adsorption–diffusion mechanism. In addition to zeolite pores, zeolite membranes with reasonable separation performance have nanometer-sized defects at the intercrystalline boundaries. The adsorption–diffusion mechanism also applies to these defects. In addition, Knudsen diffusion contributes to transport through pores larger than about 2 nm.[84] Understanding fundamental factors, such as adsorption, diffusivity, and defect properties, and incorporating them into transport models allow membrane performance to be predicted.

Liquid mixture adsorption on zeolite crystals is important for understanding and predicting pervaporation separation.[59] Li et al.[85] measured adsorption of low concentrations of methyl *tert*-butyl ether (MTBE, $C_5H_{12}O$) in water on β zeolites by measuring MTBE concentration changes after adsorption. An all-silica β zeolite was more effective in removing MTBE in water than H- and dealuminated β zeolites, because of its higher hydrophobicity, as indicated by the ratio of adsorbed 2-proponal to water at an activity of 0.9. However, this method cannot be readily applied to measure liquid mixture adsorption in zeolites, when both components in a binary mixture adsorb and/or they have similar concentrations in the liquid phase.

TABLE 2. *n*-C_6 and 3-Methylpentane (3-MP) Adsorption in MFI Zeolite (Silicalite-1) (294 K)[83]

	amount adsorbed, mol/uc	
	n-C_6	3-MP
pure component		
n-C_6	8.20	
3-MP		6.74
mol % n-C_6 in liquid		
4.70	6.32	1.34
26.0	8.20	0.04
47.1	8.25	0.04

Yu and co-workers[82,83,86] developed a density bottle method to measure amounts of liquid mixtures adsorbed in zeolite crystals, and mixture isotherms were used to analyze pervaporation results. Their measurements showed that, for *n*-hexane/3-methylpentane (MP) mixtures, *n*-hexane preferentially adsorbed to such an extent that for even for 74% MP in the liquid essentially no MP adsorbed in silicalite-1[83] (Table 2). Simulations predicted this behavior and attributed it to configurational entropy effects.[87] 2,2-Dimethylbutane (critical diameter 0.63 nm) adsorbed from the liquid phase into MFI zeolite crystals slowly at 295 K, but it was displaced from MFI crystals by *n*-hexane 3 orders of magnitude faster, perhaps due to MFI crystal expansion by *n*-hexane.[83,82] They also found that for benzene/*n*-alkane mixture adsorption, *n*-alkanes (*n*-C_6 to *n*-C_8) selectively adsorbed in silicalite-1 because *n*-alkanes have higher heats of adsorption and higher configurational entropy, whereas benzene selectively adsorbed in NaX zeolite because benzene has a higher heat of adsorption and higher saturation loading (higher entropy) in NaX super cages.[86]

Gardner and co-workers[88–92] developed a transient method to rapidly measure adsorption/diffusion properties of zeolite membranes, and to also estimate the effective membrane thickness nondestructively. Permeate responses to step changes in feed concentrations were measured, and the transport was modeled as Maxwell–Stefan diffusion with single-site Langmuir adsorption in the zeolite. Their

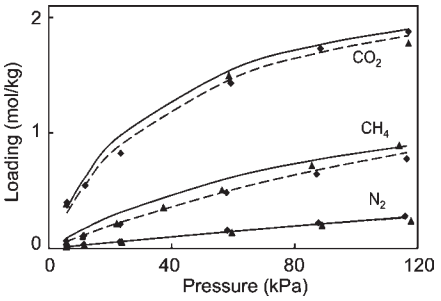

FIGURE 14. Adsorption isotherms for ZSM-5 powders by calorimetry (solid lines) and membranes by transient permeation technique (dashed lines). Experimental points are for two membranes. Reproduced with permission from ref 88. Copyright 2002 Elsevier.

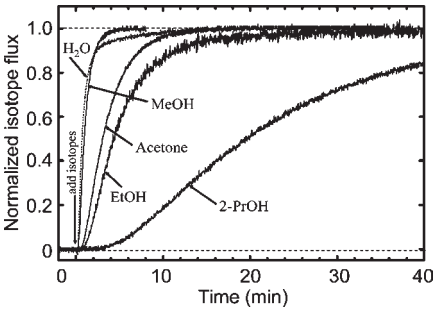

FIGURE 15. Normalized isotope permeate responses for steady-state pervaporation of pure components through a Ge-ZSM-5 zeolite membrane at 313 K. Reproduced with permission from ref 67. Copyright 2004 Elsevier.

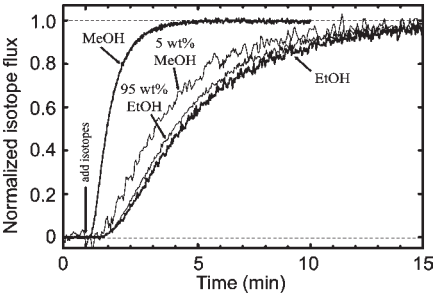

FIGURE 16. Normalized isotope permeate responses for steady-state pervaporation of methanol, ethanol, and a 95 wt % ethanol/methanol mixture through a Ge-ZSM-5 zeolite membrane (313 K). Methanol response for the mixture was smoothed, and noise in the original signal was about twice that shown here. Reproduced with permission from ref 67. Copyright 2004 Elsevier.

method also included support resistance and was valid for high loadings. Adsorption isotherms measured for N_2, CO_2, and CH_4 by transient membrane permeation through a H-ZSM-5 membrane were nearly identical to those measured by calorimetry on H-ZSM-5 crystals[88,89] (Figure 14), and butane isomer isotherms were similar to those on MFI powders. The heats of adsorption and diffusion activation energies were in the same ranges reported in the literature.[88,90] They concluded that similarity of membrane and powder isotherms indicates that these molecules diffused mainly through zeolite pores. Adsorption isotherms and butane isomers diffusivities in the transport pathways through Al-ZSM-11, Al-ZSM-5, and B-ZSM-5 zeolite membranes were also measured by transient permeation, and transient responses were modeled as Maxwell–Stefan surface diffusion with dual-site Langmuir adsorption.[92]

A transient isotopic permeation method was developed to directly measure diffusion rates under steady-state pervaporation conditions.[67,93,94] Labeled molecules were added to the feed during steady-state pervaporation, and their transient permeate responses were measured by mass spectropscopy. Bowen et al.[67] measured pure-component, isotopic transient responses through a Ge-ZSM membrane (Figure 15). They found that, at 313 K, methanol diffused at approximately the same rate as water, but 3.3, 4.8, and 20 times faster than acetone, ethanol, and 2-propanol, respectively, as determined by their lag times. Apparent diffusivities calculated from lag times and membrane thickness were on the same order as transport diffusivities reported in the literature using uptake and chromatography methods. They also found that in a methanol/ethanol mixture, ethanol inhibited methanol diffusion and methanol sped up ethanol diffusion (Figure 16). Yu et al.[94] also found similar mixture diffusion behavior for methanol/2-proponal mixtures using the same technique. This behavior is consistent with Maxwell–Stefan model predictions. However, they later found coadsorbed molecules in a ZSM-5 zeolite could decrease the diffusion rates of each other at high coverages; for an acetone/methanol mixture, both molecules diffused slower than pure acetone, which is the slower diffusing molecule.[93,94] This behavior could not be explained by the Maxwell–Stefan model. They speculated that different coverage dependencies of methanol and acetone diffusivities might lead to both molecules slowing down in the mixture, but more information is needed to understand this behavior.

Membrane separation performance (flux and selectivity) and transient permeation behavior could be predicted if adsorption and diffusion data, from either simulations or experimental measurements, are available and incorporated into appropriate transport models, such as those of Fick and Maxwell–Stefan. Fitting experimental permeation data using transport models could lead to improved understanding of permeation mechanisms and better predictions for other mixtures. We used various methods to predict permeation behaviors and explain observed permeation results through zeolite membranes, including

atomic simulations[95,96] and Maxwell–Stefan diffusion model.[40,41,94,97–99]

4. Future Directions

Permeation of molecules that are too large to adsorb in MFI pores can be used to estimate defect sizes by determining the thermodynamic activity where they undergo capillary condensation at zero-pressure drop. The flux of large molecules, however, does not help estimate the fraction of flow of other molecules through defects. Permporosimetry measurements with different molecules can determine the fraction of flux through defects and how much adsorption-induced expansion or contraction changes the flow through defects. This requires that one adsorbate expands MFI crystals (e.g., *n*-hexane) and the other causes little or no change (e.g., benzene). Such characterization studies may be useful for evaluating membrane quality prepared by other methods.[100,101]

BIOGRAPHICAL INFORMATION

Miao Yu is an Assistant Research Professor in Chemical Engineering at the University of Colorado. His Chemical Engineering degrees are from Tianjin University (B.S. 1998, M.S. 2002) and University of Colorado (Ph.D., 2007). His recent research work focuses on nanostructured membranes for separation, novel applications of carbon nanotubes, and solar cells.

Richard D. Noble is the Alfred T. and Betty E. Look Professor of Chemical Engineering at the University of Colorado. He received his B.E. and M.E degrees from Stevens Institute of Technology and his Ph.D. from UC Davis. His recent research interests include separations involving zeolite membranes, ionic liquids, and membranes.

John L. Falconer is the Mel and Virginia Clark Professor of Chemical and Biological Engineering and a President's Teaching Scholar at the University of Colorado. He received his B.S. from Johns Hopkins University and his Ph.D. from Stanford University. His research interests include zeolite membranes, heterogeneous catalysis, photocatalysis, and atomic and molecular deposition.

National Science Foundation Grants CTS-9908796, CTS-0340563, and CTS-0730047 as well as financial support by a grant (AC3-101-01) from Carbon Dioxide Reduction & Sequestration Research Center, one of 21st Century Frontier Programs funded by the Ministry of Science and Technology of Korean government.

FOOTNOTES

*To whom correspondence should be addressed. E-mail: Nobler@colorado.edu (R.D.N.); Miao.Yu@colorado.edu (M.Y.).

REFERENCES

1 Baertsch, C. D.; Funke, H. H.; Falconer, J. L.; Noble, R. D. Permeation of aromatic hydrocarbon vapors through silicalite-zeolite membranes. *J. Phys. Chem.* **1996**, *100*, 7676–7679.

2 Funke, H. H.; Kovalchick, M. G.; Falconer, J. L.; Noble, R. D. Separation of hydrocarbon isomer vapors with silicalite zeolite membranes. *Ind. Eng. Chem. Res.* **1996**, *35*, 1575–1582.

3 Coronas, J.; Noble, R. D.; Falconer, J. L. Separations of C_4 and C_6 isomers in ZSM-5 tubular membranes. *Ind. Eng. Chem. Res.* **1998**, *37*, 166–176.

4 Gump, C. J.; Noble, R. D.; Falconer, J. L. Separation of hexane isomers through nonzeolite pores in ZSM-5 zeolite membranes. *Ind. Eng. Chem. Res.* **1999**, *38*, 2775–2781.

5 Flanders, C. L.; Tuan, V. A.; Noble, R. D.; Falconer, J. L. Separation of C_6 isomers by vapor permeation and pervaporation through ZSM-5 membranes. *J. Membr. Sci.* **2000**, *176*, 43–53.

6 Funke, H. H.; Argo, A. M.; Baertsch, C. D.; Falconer, J. L.; Noble, R. D. Separation of close-boiling hydrocarbons with silicalite zeolite membranes. *J. Chem. Soc., Faraday Trans.* **1996**, *92*, 2499–2502.

7 Hong, M.; Falconer, J. L.; Noble, R. D. Modification of zeolite membranes for H_2 separation by catalytic cracking of methyldiethoxysilane. *Ind. Eng. Chem. Res.* **2005**, *44*, 4035–4041.

8 Li, S. G.; Falconer, J. L.; Noble, R. D. Improved SAPO-34 membranes for CO_2/CH4 separations. *Adv. Mater.* **2006**, *18*, 2601–2603.

9 Kalipcilar, H.; Falconer, J. L.; Noble, R. D. Preparation of B-ZSM-5 membranes on a monolith support. *J. Membr. Sci.* **2001**, *194*, 141–144.

10 Jia, M. D.; Chen, B. S.; Noble, R. D.; Falconer, J. L. Ceramic-zeolite composite membranes and their application for separation of vapor gas-mixtures. *J. Membr. Sci.* **1994**, *90*, 1–10.

11 Bai, C. S.; Jia, M. D.; Falconer, J. L.; Noble, R. D. Preparation and separation properties of silicalite composite membranes. *J. Membr. Sci.* **1995**, *105*, 79–87.

12 Noble, R. D.; Falconer, J. L. Silicalite-1 zeolite composite membranes. *Catal. Today* **1995**, *25*, 209–212.

13 Funke, H. H.; Argo, A. M.; Falconer, J. L.; Noble, R. D. Separations of cyclic, branched, and linear hydrocarbon mixtures through silicalite membranes. *Ind. Eng. Chem. Res.* **1997**, *36*, 137–143.

14 Funke, H. H.; Frender, K. R.; Green, K. M.; Wilwerding, J. L.; Sweitzer, B. A.; Falconer, J. L.; Noble, R. D. Influence of adsorbed molecules on the permeation properties of silicalite membranes. *J. Membr. Sci.* **1997**, *129*, 77–82.

15 Liu, Q.; Noble, R. D.; Falconer, J. L.; Funke, H. H. Organics/water separation by pervaporation with a zeolite membrane. *J. Membr. Sci.* **1996**, *117*, 163–174.

16 Coronas, J.; Falconer, J. L.; Noble, R. D. Characterization and permeation properties of ZSM-5 tubular membranes. *AIChE J.* **1997**, *43*, 1797–1812.

17 Lin, X.; Falconer, J. L.; Noble, R. D. Parallel pathways for transport in ZSM-5 zeolite membranes. *Chem. Mater.* **1998**, *10*, 3716–3723.

18 Tuan, V. A.; Falconer, J. L.; Noble, R. D. Alkali-free ZSM-5 membranes: Preparation conditions and separation performance. *Ind. Eng. Chem. Res.* **1999**, *38*, 3635–3646.

19 Aoki, K.; Tuan, V. A.; Falconer, J. L.; Noble, R. D. Gas permeation properties of ion-exchanged ZSM-5 zeolite membranes. *Microporous Mesoporous Mater.* **2000**, *39*, 485–492.

20 Gump, C. J.; Lin, X.; Falconer, J. L.; Noble, R. D. Experimental configuration and adsorption effects on the permeation of C-4 isomers through ZSM-5 zeolite membranes. *J. Membr. Sci.* **2000**, *173*, 35–52.

21 Tuan, V. A.; Falconer, J. L.; Noble, R. D. Isomorphous substitution of Al, Fe, B, and Ge into MFI-zeolite membranes. *Microporous Mesoporous Mater.* **2000**, *41*, 269–280.

22 Tuan, V. A.; Noble, R. D.; Falconer, J. L. Boron-substituted ZSM-5 membranes: Preparation and separation performance. *AIChE J.* **2000**, *46*, 1201–1208.

23 Gade, S. K.; Tuan, V. A.; Gump, C. J.; Noble, R. D.; Falconer, J. L. Highly selective separation of n-hexane from branched, cyclic and aromatic hydrocarbons using B-ZSM-5 membranes. *Chem. Commun.* **2001**, 601–602.

24 Li, S. G.; Tuan, V. A.; Falconer, J. L.; Noble, R. D. Separation of 1,3-propanediol from glycerol and glucose using a ZSM-5 zeolite membrane. *J. Membr. Sci.* **2001**, *191*, 53–59.

25 Li, S. G.; Tuan, V. A.; Noble, R. D.; Falconer, J. L. A Ge-substituted ZSM-5 zeolite membrane for the separation of acetic acid from water. *Ind. Eng. Chem. Res.* **2001**, *40*, 6165–6171.

26 Bowen, T. C.; Kalipcilar, H.; Falconer, J. L.; Noble, R. D. Separation of C_4 and C_6 isomer mixtures and alcohol-water solutions by monolith supported B-ZSM-5 membranes. *Desalination* **2002**, *147*, 331–332.

27 Bowen, T. C.; Li, S. G.; Tuan, V. A.; Falconer, J. L.; Noble, R. D. Pervaporation of aqueous organic mixtures through Ge-ZSM-5 zeolite membranes. *Desalination* **2002**, *147*, 327–329.

28 Kalipcilar, H.; Gade, S. K.; Noble, R. D.; Falconer, J. L. Synthesis and separation properties of B-ZSM-5 zeolite membranes on monolith supports. *J. Membr. Sci.* **2002**, *210*, 113–127.

29 Tuan, V. A.; Li, S. G.; Falconer, J. L.; Noble, R. D. Separating organics from water by pervaporation with isomorphously-substituted MFI zeolite membranes. *J. Membr. Sci.* **2002**, *196*, 111–123.

30 Bowen, T. C.; Kalipcilar, H.; Falconer, J. L.; Noble, R. D. Pervaporation of organic/water mixtures through B-ZSM-5 zeolite membranes on monolith supports. *J. Membr. Sci.* **2003**, *215*, 235–247.

31 Li, S.; Tuan, V. A.; Falconer, J. L.; Noble, R. D. Properties and separation performance of Ge-ZSM-5 membranes. *Microporous Mesoporous Mater.* **2003**, *58*, 137–154.

32 Yan, Y. S.; Davis, M. E.; Gavalas, G. R. Preparation of zeolite ZSM-5 Membranes by in-situ crystallization on porous α-Al_2O_3. *Ind. Eng. Chem. Res.* **1995**, *34*, 1652–1661.

33 Motuzas, J.; Julbe, A.; Noble, R. D.; Guizard, C.; Beresnevicius, Z. J.; Cot, D. Rapid synthesis of silicalite-1 seeds by microwave assisted hydrothermal treatment. *Microporous Mesoporous Mater.* **2005**, *80*, 73–83.

34 Poshusta, J. C.; Tuan, V. A.; Falconer, J. L.; Noble, R. D. Synthesis and permeation properties of SAPO-34 tubular membranes. *Ind. Eng. Chem. Res.* **1998**, *37*, 3924–3929.

35 Poshusta, J. C.; Tuan, V. A.; Pape, E. A.; Noble, R. D.; Falconer, J. L. Separation of light gas mixtures using SAPO-34 membranes. *AIChE J.* **2000**, *46*, 779–789.

36 Poshusta, J. C.; Noble, R. D.; Falconer, J. L. Characterization of SAPO-34 membranes by water adsorption. *J. Membr. Sci.* **2001**, *186*, 25–40.

37 Li, S. G.; Falconer, J. L.; Noble, R. D. SAPO-34 membranes for CO_2/CH_4 separation. *J. Membr. Sci.* **2004**, *241*, 121–135.

38 Li, S. G.; Alvarado, G.; Noble, R. D.; Falconer, J. L. Effects of impurities on CO_2/CH_4 separations through SAPO-34 membranes. *J. Membr. Sci.* **2005**, *251*, 59–66.

39 Li, S. G.; Martinek, J. G.; Falconer, J. L.; Noble, R. D.; Gardner, T. Q. High-pressure CO_2/CH_4 separation using SAPO-34 membranes. *Ind. Eng. Chem. Res.* **2005**, *44*, 3220–3228.

40 Li, S. G.; Falconer, J. L.; Noble, R. D.; Krishna, R. Modeling permeation of CO_2/CH_4, CO_2/N_2, and N_2/CH_4 mixtures across SAPO-34 membrane with the Maxwell−Stefan equations. *Ind. Eng. Chem. Res.* **2007**, *46*, 3904–3911.

41 Li, S. G.; Falconer, J. L.; Noble, R. D.; Krishna, R. Interpreting unary, binary, and ternary mixture permeation across a SAPO-34 membrane with loading-dependent Maxwell−Stefan diffusivities. *J. Phys. Chem. C* **2007**, *111*, 5075–5082.

42 Carreon, M. A.; Li, S. G.; Falconer, J. L.; Noble, R. D. Alumina-supported SAPO-34 membranes for CO_2/CH_4 separation. *J. Am. Chem. Soc.* **2008**, *130*, 5412–5413.

43 Carreon, M. A.; Li, S. G.; Falconer, J. L.; Noble, R. D. SAPO-34 seeds and membranes prepared using multiple structure directing agents. *Adv. Mater.* **2008**, *20*, 729–732.

44 Li, S. G.; Carreon, M. A.; Zhang, Y. F.; Funke, H. H.; Noble, R. D.; Falconer, J. L. Scale-up of SAPO-34 membranes for CO_2/CH_4 separation. *J. Membr. Sci.* **2010**, *352*, 7–13.

45 Li, S. G.; Falconer, J. L.; Noble, R. D. SAPO-34 membranes for CO_2/CH_4 separations: Effect of Si/Al ratio. *Microporous Mesoporous Mater.* **2008**, *110*, 310–317.

46 Lok, B. M.; Messina, C. A.; Patton, R. L.; Gajek, R. T.; Cannan, T. R.; Flanigen, E. M. Crystalline Silicoalumino Phosphates. U.S. Patent, Number 5370851, 1984.

47 Zhang, Y. F.; Tokay, B.; Funke, H. H.; Falconer, J. L.; Noble, R. D. Template removal from SAPO-34 crystals and membranes. *J. Membr. Sci.* **2010**, *363*, 29–35.

48 Gump, C. J.; Tuan, V. A.; Noble, R. D.; Falconer, J. L. Aromatic permeation through crystalline molecular sieve membranes. *Ind. Eng. Chem. Res.* **2001**, *40*, 565–577.

49 Li, S. G.; Tuan, V. A.; Falconer, J. L.; Noble, R. D. Separation of 1,3-propanediol from aqueous solutions using pervaporation through an X-type zeolite membrane. *Ind. Eng. Chem. Res.* **2001**, *40*, 1952–1959.

50 Li, S. G.; Tuan, V. A.; Noble, R. D.; Falconer, J. L. Pervaporation of water/THF mixtures using zeolite membranes. *Ind. Eng. Chem. Res.* **2001**, *40*, 4577–4585.

51 Tuan, V. A.; Li, S. G.; Noble, R. D.; Falconer, J. L. Preparation and pervaporation properties of a MEL-type zeolite membrane. *Chem. Commun.* **2001**, 583–584.

52 Kalipcilar, H.; Bowen, T. C.; Noble, R. D.; Falconer, J. L. Synthesis and separation performance of SSZ-13 zeolite membranes on tubular supports. *Chem. Mater.* **2002**, *14*, 3458–3464.

53 Li, S.; Tuan, V. A.; Falconer, J. L.; Noble, R. D. X-type zeolite membranes: preparation, characterization, and pervaporation performance. *Microporous Mesoporous Mater.* **2002**, *53*, 59–70.

54 Li, S. G.; Tuan, V. A.; Noble, R. D.; Falconer, J. L. ZSM-11 membranes: Characterization and pervaporation performance. *AIChE J.* **2002**, *48*, 269–278.

55 Tuan, V. A.; Li, S. G.; Falconer, J. L.; Noble, R. D. In situ crystallization of β zeolite membranes and their permeation and separation properties. *Chem. Mater.* **2002**, *14*, 489–492.

56 Tuan, V. A.; Weber, L. L.; Falconer, J. L.; Noble, R. D. Synthesis of B-substituted beta-zeolite membranes. *Ind. Eng. Chem. Res.* **2003**, *42*, 3019–3021.

57 Bein, T. Synthesis and applications of molecular sieve layers and membranes. *Chem. Mater.* **1996**, *8*, 1636–1653.

58 Caro, J.; Noack, M.; Kolsch, P.; Schafer, R. Zeolite membranes - state of their development and perspective. *Microporous Mesoporous Mater.* **2000**, *38*, 3–24.

59 Bowen, T. C.; Noble, R. D.; Falconer, J. L. Fundamentals and applications of pervaporation through zeolite membranes. *J. Membr. Sci.* **2004**, *245*, 1–33.

60 McLeary, E. E.; Jansen, J. C.; Kapteijn, F. Zeolite based films, membranes and membrane reactors: progress and prospects. *Microporous Mesoporous Mater.* **2006**, *90*, 198–220.

61 Caro, J.; Noack, M. Zeolite membranes - recent developments and progress. *Microporous Mesoporous Mater.* **2008**, *115*, 215–233.

62 Lew, C. M.; Cai, R.; Yan, Y. S. Zeolite thin films: from computer chips to space stations. *Acc. Chem. Res.* **2010**, *43*, 210–219.

63 Coronas, J.; Santamaria, J. Separations using zeolite membranes. *Sep. Purif. Methods* **1999**, *28*, 127–177.

64 Coronas, J.; Santamaria, J. The use of zeolite films in small-scale and micro-scale applications. *Chem. Eng. Sci.* **2004**, *59*, 4879–4885.

65 Smetana, J. F.; Falconer, J. L.; Noble, R. D. Separation of methyl ethyl ketone from water by pervaporation using a silicalite membrane. *J. Membr. Sci.* **1996**, *114*, 127–130.

66 Motuzas, J.; Julbe, A.; Noble, R. D.; van der Lee, A.; Beresnevicius, Z. J. Rapid synthesis of oriented silicalite-1 membranes by microwave-assisted hydrothermal treatment. *Microporous Mesoporous Mater.* **2006**, *92*, 259–269.

67 Bowen, T. C.; Wyss, J. C.; Noble, R. D.; Falconer, J. L. Measurements of diffusion through a zeolite membrane using isotopic-transient pervaporation. *Microporous Mesoporous Mater.* **2004**, *71*, 199–210.

68 Yu, M.; Amundsen, T. J.; Hong, M.; Falconer, J. L.; Noble, R. D. Flexible nanostructure of MFI zeolite membranes. *J. Membr. Sci.* **2007**, *298*, 182–189.

69 Yu, M.; Falconer, J. L.; Amundsen, T. J.; Hong, M.; Noble, R. D. A controllable nanometer-sized valve. *Adv. Mater.* **2007**, *19*, 3032–3036.

70 Sommer, S.; Melin, T.; Falconer, J. L.; Noble, R. D. Transport of C_6 isomers through ZSM-5 zeolite membranes. *J. Membr. Sci.* **2003**, *224*, 51–67.

71 Arruebo, M.; Falconer, J. L.; Noble, R. D. Separation of binary C_5 and C_6 hydrocarbon mixtures through MF1 zeolite membranes. *J. Membr. Sci.* **2006**, *269*, 171–176.

72 Yu, M.; Falconer, J. L.; Noble, R. D. Characterizing nonzeolitic pores in MFI membranes. *Ind. Eng. Chem. Res.* **2008**, *47*, 3943–3948.

73 Lee, J. B.; Funke, H. H.; Noble, R. D.; Falconer, J. L. High selectivities in defective MFI membranes. *J. Membr. Sci.* **2008**, *321*, 309–315.

74 Sorenson, S. G.; Smyth, J. R.; Kocirik, M.; Zikanova, A.; Noble, R. D.; Falconer, J. L. Adsorbate-induced expansion of silicalite-1 crystals. *Ind. Eng. Chem. Res.* **2008**, *47*, 9611–9616.

75 Lee, J. B.; Funke, H. H.; Noble, R. D.; Falconer, J. L. Adsorption-induced expansion of defects in MFI membranes. *J. Membr. Sci.* **2009**, *341*, 238–245.

76 Sorenson, S. G.; Smyth, J. R.; Noble, R. D.; Falconer, J. L. Correlation of crystal lattice expansion and membrane properties for MFI zeolites. *Ind. Eng. Chem. Res.* **2009**, *48*, 10021–10024.

77 Tokay, B.; Falconer, J. L.; Noble, R. D. Alcohol and water adsorption and capillary condensation in MFI zeolite membranes. *J. Membr. Sci.* **2009**, *334*, 23–29.

78 Gibbons, W. T.; Zhang, Y. F.; Falconer, J. L.; Noble, R. D. Inhibiting crystal swelling in MFI zeolite membranes. *J. Membr. Sci.* **2010**, *357*, 54–61.

79 Sorenson, S. G.; Payzant, E. A.; Noble, R. D.; Falconer, J. L. Influence of crystal expansion/contraction on zeolite membrane permeation. *J. Membr. Sci.* **2010**, *357*, 98–104.

80 Yu, M.; Falconer, J. L.; Noble, R. D. Characterizing non-zeolitic pore volume in zeolite membranes by temperature-programmed desorption. *Microporous Mesoporous Mater.* **2008**, *113*, 224–230.

81 Sorenson, G. S.; Payzant, E. A.; Gibbons, W. T.; Soydas, B.; Kita, H.; Noble, R. D.; Falconer, J. L. Influence of zeolite crystal expansion/contraction on NaA zeolite membrane separations. *J. Membr. Sci.* **2011**, *366*, 413–420.

82 Yu, M.; Wyss, J. C.; Noble, R. D.; Falconer, J. L. 2,2-Dimethylbutane adsorption and diffusion in MFI zeolite. *Microporous Mesoporous Mater.* **2008**, *111*, 24–31.

83 Yu, M.; Falconer, J. L.; Noble, R. D. Adsorption of liquid mixtures on silicalite-1 zeolite: A density-bottle method. *Langmuir* **2005**, *21*, 7390–7397.

84 denExter, M. J.; Jansen, J. C.; vandeGraaf, J. M.; Kapteijn, F.; Moulijn, J. A.; vanBekkum, H. Zeolite-based membranes preparation, performance and prospect. *Stud. Surf. Sci. Catal.* **1996**, *102*, 413–454.

85 Li, S. G.; Tuan, V. A.; Noble, R. D.; Falconer, J. L. MTBE adsorption on all-silica beta zeolite. *Environ. Sci. Technol.* **2003**, *37*, 4007–4010.

86 Yu, M.; Hunter, J. T.; Falconer, J. L.; Noble, R. D. Adsorption of benzene mixtures on silicalite-1 and NaX zeolites. *Microporous Mesoporous Mater.* **2006**, *96*, 376–385.

87 Calero, S.; Smit, B.; Krishna, R. Configurational entropy effects during sorption of hexane isomers in silicalite. *J. Catal.* **2001**, *202*, 395–401.

88 Gardner, T. Q.; Falconer, J. L.; Noble, R. D. Adsorption and diffusion properties of zeolite membranes by transient permeation. *Desalination* **2002**, *149*, 435–440.

89 Gardner, T. Q.; Flores, A. I.; Noble, R. D.; Falconer, J. L. Transient measurements of adsorption and diffusion in H-ZSM-5 membranes. *AIChE J.* **2002**, *48*, 1155–1167.

90 Gardner, T. Q.; Lee, J. B.; Noble, R. D.; Falconer, J. L. Adsorption and diffusion properties of butanes in ZSM-5 zeolite membranes. *Ind. Eng. Chem. Res.* **2002**, *41*, 4094–4105.

91 Gardner, T. Q.; Falconer, J. L.; Noble, R. D.; Zieverink, M. M. P. Analysis of transient permeation fluxes into and out of membranes for adsorption measurements. *Chem. Eng. Sci.* **2003**, *58*, 2103–2112.

92 Gardner, T. Q.; Falconer, J. L.; Noble, R. D. Transient permeation of butanes through ZSM-5 and ZSM-11 zeolite membranes. *AIChE J.* **2004**, *50*, 2816–2834.

93 Bowen, T. C.; Wyss, J. C.; Noble, R. D.; Falconer, J. L. Inhibition during multicomponent diffusion through ZSM-5 zeolite. *Ind. Eng. Chem. Res.* **2004**, *43*, 2598–2601.

94 Yu, M.; Falconer, J. L.; Noble, R. D.; Krishna, R. Modeling transient permeation of polar organic mixtures through a MFI zeolite membrane using the Maxwell–Stefan equations. *J. Membr. Sci.* **2007**, *293*, 167–173.

95 Bowen, T. C.; Falconer, J. L.; Noble, R. D.; Skoulidas, A. I.; Sholl, D. S. A comparison of atomistic simulations and experimental measurements of light gas permeation through zeolite membranes. *Ind. Eng. Chem. Res.* **2002**, *41*, 1641–1650.

96 Skoulidas, A. I.; Bowen, T. C.; Doelling, C. M.; Falconer, J. L.; Noble, R. D.; Sholl, D. S. Comparing atomistic simulations and experimental measurements for CH_4/CF_4 mixture permeation through silicalite membranes. *J. Membr. Sci.* **2003**, *227*, 123–136.

97 Krishna, R.; Li, S.; van Baten, J. M.; Falconer, J. L.; Noble, R. D. Investigation of slowing-down and speeding-up effects in binary mixture permeation across SAPO-34 and MFI membranes. *Sep. Purif. Technol.* **2008**, *60*, 230–236.

98 Martinek, J. G.; Gardner, T. Q.; Noble, R. D.; Falconer, J. L. Modeling transient permeation of binary mixtures through zeolite membranes. *Ind. Eng. Chem. Res.* **2006**, *45*, 6032–6043.

99 Gardner, T. Q.; Martinek, J. G.; Falconer, J. L.; Noble, R. D. Enhanced flux through double-sided zeolite membranes. *J. Membr. Sci.* **2007**, *304*, 112–117.

100 Lai, Z. P.; Bonilla, G.; Diaz, I.; Nery, J. G.; Sujaoti, K.; Amat, M. A.; Kokkoli, E.; Terasaki, O.; Thompson, R. W.; Tsapatsis, M.; Vlachos, D. G. Microstructural optimization of a zeolite membrane for organic vapor separation. *Science* **2003**, *300*, 456–460.

101 Choi, J.; Jeong, H. K.; Snyder, M. A.; Stoeger, J. A.; Masel, R. I.; Tsapatsis, M. Grain Boundary Defect Elimination in a Zeolite Membrane by Rapid Thermal Processing. *Science* **2009**, *325*, 590–593.

102 International Zeolite Association, http://www.iza-structure.org/default.htm.